Progress In Electromagnetics Research C, Vol. 67, 173–184, 2016

A New Method of Driving Wire Dipole Antennas to Multiband Operation via Non-Uniform EBG Lattices for Employment to Wireless Communication Applications

Christos Mourtzios and Katherine Siakavara*

Abstract—In this paper, a novel approach is attained to the design of low profile antenna structures with wire dipoles and multiband operation. The aim is achieved by utilization of non-uniform Electromagnetic Band Gap (EBG) lattices as reflectors, and this potential comes to be added to the total of special capabilities of this type of Artificial Magnetic Conductors (AMC). It is proved that a properly designed EBG of this type can resonate at more than one frequency and is capable to drive, inside these bands, the dipole to higher order modes of operation besides its basic one. The resulting hybrid radiator apart from its multiband operation exhibits high gain that reaches the value of 9.6 dB, satisfactory Mean Effective Gain (MEG) and very low correlation coefficients, much less than 0.1, between the signals at the input of the dipoles in the case that the radiator is configured as an antenna array. The study of these quantities was performed using the signal characteristics of a real mobile communication environment along with the hybrid antenna properties of operation. The presented analytical results show that the designed radiators are competitive to the classical microstrip ones and can be effectively used in modern wireless communication networks, incorporated either into stationary or into mobile units.

1. INTRODUCTION

Modern-age wireless/mobile networks are required to offer a great variety of communication services, and consequently they have to operate at multiple frequency bands. The devices, mobile or not, which serve such systems, are products of high technology, designed to operate in accordance to communication protocols used. The antennas, incorporated into this equipment and generally into large systems as the base stations of communication networks, being the units which transform the processed communication signals from currents to radiated waves, are crucial for the correct and efficient operation of the entire network. However, their design is not an easy task. Ordinary requirements that they have to meet are multiband operation, high gain and efficiency, satisfactory MEG, low correlation coefficient between the signal channels of the array elements in the case of Multiple Input Multiple Output (MIMO) applications, etc. All these attributes have to be ensured usually with compact antennas with small size and low profile.

The most popular type of antennas with the above attributes are microstrip or printed antennas, and a great variety of methods for design and incorporating them into modern devices have been proposed in the literature. All of these methods lead to radiating schemes with effective operation. An alternative antenna type, suitable for modern applications, is classical linear wire dipole which is superior to the microstrip ones regarding the much higher power level that can handle but lacks in other features as

Received 18 July 2016, Accepted 14 September 2016, Scheduled 27 September 2016
* Corresponding author: Katherine Siakavara (skv@physics.auth.gr).
The authors are with the Radiocommunications Laboratory, School of Physics, Aristotle University of Thessaloniki, Thessaloniki 54124, Greece.

size, not low profile when combined with a reflector, single frequency band of operation, relatively low gain, etc. However, recently novel and efficient techniques to design wire dipole antenna structures, with very low profile, controllable and perhaps high gain, and some other attributes of operation suitable for mobile networking, have been proposed by researchers. A major category of them includes hybrid systems composed of dipoles the operation of which is enhanced by EBG lattices positioned in close proximity to them. In accordance to the literature, hybrid 'antenna-EBG' structures would have gain and frequency bandwidth larger than that of simple antennas, specific radiation patterns regarding the space distribution of the radiated power, satisfactory Front-to Back Ratio, etc, and at the same time be miniaturized and of very low profile [1–6]. Additionally, attributes as polarization diversity, sufficient MEG and reduction of mutual coupling between the antenna array elements could be obtained, thus being attractive to modern applications [7–12]. Recently, a novel configuration for EBG lattices has been proposed in the literature. It differs from the ordinary one, as the usual EBGs are periodic configurations of identical printed patches while the new EBG lattice is non-uniform, namely is not periodic, as composed of patches non-identical, with size gradually reduced via a specific scaling factor. They were initially applied to beam tilting of base station antennas [13], antenna beam steering [14] or realizing flat parabola antennas [15]. Further investigation proved that this EBG type was more robust than the classical one, in the enhancement of antennas' characteristics of operation. In [16–19], it was found that when EBGs were combined with simple linear dipoles, positioned very close to the EBG, antenna arrays with high gain are obtained, at the frequency of resonance. It was also shown that the values of these indices are more satisfactory than the respective ones of dipole arrays without any reflector, or when a Perfect Electric Conductor (PEC) or a uniform EBG surface is used as a reflector.

In the present work, the effect of a non-uniform EBG structure on the operation of a wire dipole is approached by another way and for another scope. It is studied if the EBG could drive the wire dipole to multiband operation. Several techniques to this aim obtained are found in the literature, especially for printed dipoles. To drive this antenna type at multi-frequency operation is easier than to do it in the case of a wire dipole, as the designer has the potential to suitably configure printed element's shape for example fractaly, or to incorporate into them metamaterial elements [20–28] thus obtaining simultaneously compact antennas with low profile. In the work at hand in accordance to the scope of utilizing wire dipoles performing at more than one frequency bands, the problem's solution was given by employing a planar nonuniform EBG in close proximity to the dipoles. The EBG lattice although operates as a passive reflecting scheme, without being fed, is substantially driven inductively by the dipoles, and if it is properly designed to resonate at specific frequencies it will in turn be capable to drive the dipoles in a type of resonance at these frequencies. These resonances do not appear in the absence of the EBG lattice as they do not result from the dipoles' length. Thus the hybrid arrangement dipoles-nonuniform EBG will work as a low profile multi-band radiating scheme with potentially specific operation features and being perhaps a good choice for modern applications. This potential is investigated in the present work and proved to be feasible.

2. THE ATTRIBUTES OF NON-UNIFORM EBGS

The EBG lattices, termed also as High Impedance Surfaces (HIS), are classified to the group of Artificial Magnetic Conductors and have gained significant attention in last decades in the designing of antennas and more generally at microwave systems as the EBG lattices will efficiently enhance the performance of antennas and microwave systems [29–32]. Their positive contribution to the advanced operation of these systems is due to their two important properties: their ability to present high impedance to a localized source or plane wave impinging onto their surface as well as the exhibition of a surface wave band-gap that prevents the wave propagation through their structure. The EBGs are usually designed such that both the above properties exist over the same frequency band even if only one of them is exploited in a specific application. The classical configuration of the EBG lattice is of mushroom type [33] composed of periodically arranged identical patches conductively connected via thin metallic pins (vias) to ground metallic sheet and a dielectric layer between the patches and the ground thus constituting a microstrip structure (Fig. 1(a)).

The specific structuring of ordinary EBG lattices differentiates their behavior to the incident waves, from that of a (PEC), causing reflection phase of 0° at the specific frequency band, for which it they are

designed, instead of the 180° reflection caused by the PEC. Namely they perform as AMC. In detail, the AMC's reflection phase varies continuously from +180° to −180°, through 0° at the surface's frequency of resonance[29]. Due to these reflection attributes when a wire dipole antenna is positioned in front of PEC and the distance PEC-dipole equal to $\lambda/4$, the optimal operation is obtained, in order to balance the 180° reflection phase. In contrast, when EBG is used, the distance EBG-dipole needs to be very small, due to the almost zero reflection phase. In this way, very low profile antenna structures will be designed.

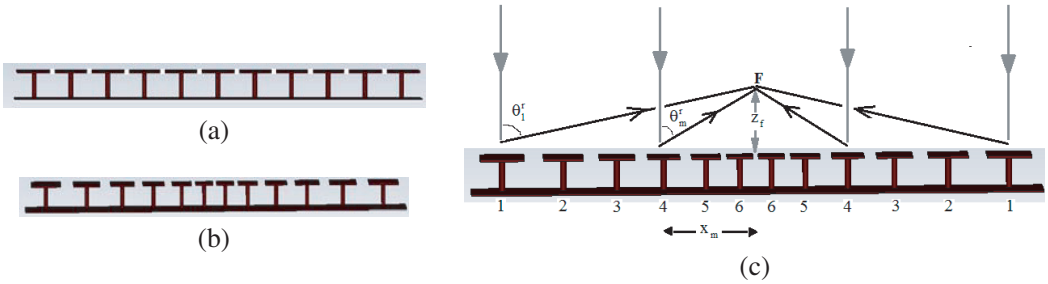

Figure 1. Profile of (a) uniform and (b) non-uniform EBG lattice and (c) the mechanism of reflection from the non-uniform that would lead to focusing of the reflected rays.

The non-uniform EBG results from the ordinary one, with identical patches, by modifying the size of the patches and their inter-distances via gradient factors [16–19]. Such a configuration is depicted in Fig. 1(b) at which six patches gradually shortened, along with their mirrors with respect to the middle of the arrangement, are illustrated. The side-lengths of mth and $(m+1)$th patches are related by a scale factor s, as $s = L_m/L_{m+1}$, while the distance g between adjacent patches changes also gradually from cell to cell by the factor g_s as $g_s = g_m/g_{m+1}$. This texturing of the EBG surface, in contrast to the uniform EBG, results in surface impedance, Z_s, variation from point to point on the lattice, which in turn leads to a gradually varying reflection phase of an impinging wave at the point of incidence, e.g., the reflection phase at the mth cell is calculated by the formula $\phi_m = \mathrm{Im}\{\ln((Z_{sm} - Z_0)(Z_{sm} + Z_0)^{-1})\}$, where Z_0 is the wave impedance in the dielectric layer above the lattice [29]. All these results lend to the non-uniform lattice, special attributes making it superior to the uniform one. In accordance with the Snell' s law, a plane wave perpendicularly impinging to a PEC is reflected perpendicularly to the surface because the reflection phase at any surface point is 180°. If the reflecting surface is textured by the way described above, the directions of the reflected rays are not perpendicular to the surface, as the reflection phase has no equal values at all surface' s points. For example, at the mth cell it is calculated by $\theta_m^r = \sin^{-1}((\Delta\phi_{m,m+1})(\beta\Delta x_{m,m+1})^{-1})$ where $\Delta x_{m,m+1}$ is the space between the middles of the mth and $(m+1)$th patches. An interesting exploitation of this attribute is a proper tuning of s and g_s to a desired θ_m^r at any surface point be obtained. This gradual variation will cause focusing of the reflected rays at a distance z_f (Fig. 1(c)) above the surface, if Eq. (1) is valid [18]. In this equation, x_m stands for the distance of the mth cell's middle from the middle of the array.

$$z_f = x_1 \tan\left(\frac{\pi}{2} - \theta^{r_1}\right) = x_2 \tan\left(\frac{\pi}{2} - \theta^{r_2}\right) = \ldots = x_m \tan\left(\frac{\pi}{2} - \theta^{r_m}\right) \quad (1)$$

3. THE EXPLOITATION OF NON-UNIFORM EBGS' PERFORMANCE

3.1. Multi-Frequency EBG-Dipole Schemes

The described mechanism of reflection at the non-uniform EBGs tends to direct the reflected rays towards the middle of the focusing EBG area. It has been proved that this fact positively influences the electromagnetic performance of a hybrid antenna array, composed of linear dipoles located over the middle of focusing areas, by two ways a) the electromagnetic energy interchange between the dipoles, is reduced resulting in small coupling between them and b) the focusing of energy will yield higher gain values of the antenna schemes [16–19].

In the present work, a new investigation is carried out with aim at additional properties of this type of hybrid schemes to be found. Particularly, the possibility of the radiator to be driven at multi-frequency operation without any new element to be added to it is examined. The synthesized and studied structure is depicted in Fig. 2. The non-uniform EBG lattice is composed of 9 rows, each one of them having 6 patches and their mirrors, thus totally 12 elements per row. The patches from 1 to 6 (Fig. 1(c)) are gradually shortened in accordance to the theory of the previous section. The size and inter-distances of the rest five out of six patches are calculated by properly selecting factors s and g_s. Although the phenomenon of focusing exists and is expected to enhance the performance of the hybrid antenna, the mathematical equations of Section 2 are not adequate to determine accurately the values of the geometrical parameters of the EBG as, a) the dipole, positioned above and very close to the EBG's surface, strongly interacts with the lattice and b) the requirement of the design is the focusing area of the 9×12 patches to resonate at more than one frequency band. So, the entire problem is complex and multi-parametric, and a global handling of the parameter values is necessary. The steps of the design are presented in detail at a following point of the section, next to the analysis of the electromagnetic behavior of the EBG focusing area. For this purpose and given that in the case of antenna arrays of N elements, N such focusing areas, one next to the other, will be used, and each one of them considered as a unit cell of a periodic array of similar focusing cells. So, each focusing area-cell is considered to have two ports as shown in Fig. 2(c), and for its electromagnetic performance analysis, the theory of periodic structures is applied no matter whether the interior of the cells is non periodic as composed of the non-identical EBG patches. In accordance to the theory, the transfer parameters A, B, C, D of the nth unit cell relate the 'input port' n, with the respective output port $(n+1)$th, that is simultaneously the input of the next cell. So, the voltage and current at the nth terminal differ from the respective ones of the $n+1$ terminal by the propagation factor $e^{-\gamma d}$. The constant γ is a complex number and constitutes an equivalent propagation coefficient which comes just from the quantitative relation between the voltages and current between the terminals and not being the actual propagation constant of the signal-wave in the interior of the cell. These interrelations are mathematically described by $V_{n+1} = V_n e^{-\gamma d}, I_{n+1} = I_n e^{-\gamma d}$. In accordance to the theory of periodic structures [34], constant γ depends on the transfer parameters of the cell — a two-port network by equation $\cosh(\gamma d) = (\dot{A} + \dot{D})/2$. A criterion of the performance of the cell versus frequency is the values of the $\gamma(f) = \alpha(f) + j\beta(f)$,

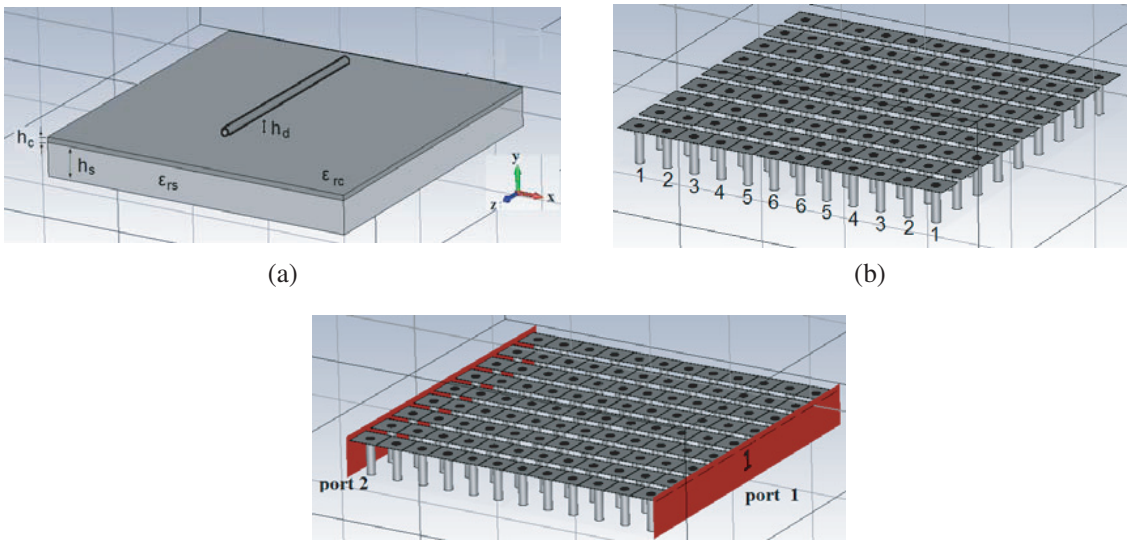

(a) (b)

(c)

Figure 2. (a) External view of the non-uniform EBG cell with dielectric cover, of constant ε_{rc} and height h_s and the dipole above it. (b) The EBG structure with the non-identical patches and the respective metallic pins embedded inside a dielectric layer of constant ε_{rs} and thickness h_s. (c) The two port EBG unit cell. Size of unit cell: 76.5 mm $\times$ 68 mm.

where $\beta(f)$ is the phase constant and physically defined as $\beta(f) = \omega/v_\phi$, with v_ϕ being the phase velocity. Zero value of $\beta(f)$ at specific frequencies means no signal propagation between the ports. In the case of EBG cells, these zeros coincide with the frequencies of resonance of the focusing area-cell and the performance of it as an AMC. Inside these frequency bands it will be expected that a dipole, positioned very close to the lattice and strongly interacting with it, will be driven in multi-frequency performance.

The performance of the EBG as a two-port network is found via simulation, with a high frequency electromagnetic solver, by which the scattering coefficients S_{ij} between the cell ports are calculated, and in turn these values are used for the calculation of the A and D parameters. The estimation of $\beta(f)$ is done by utilization of the equation, mentioned previously, which relates it with the A and D parameters. From the equation and via some mathematical manipulations, the formula of Eq. (2) is resulted

$$\beta(f) = a \sin\left(p(f) \cdot w(f)^{-1}\right) \cdot d_{cell}^{-1} \tag{2}$$

where $p(f) = \mathrm{Im}((A(f) + D(f))/2)d_{cell}$ is the length of the focusing area-unit cell, $w(f) = (-q(f) + (q(f)^2 + 4\,p(f)^2)^{1/2}) \cdot 2^{-1}$ and $q(f) = 1 - (\mathrm{Re}((A(f) + D(f))/2))^2 - p(f)^2$. The parameters A and D are calculated directly by the simulated $S_{ij}(f)$ values and via the mathematical types [34]: $A(f) = [(1 + S_{11})(1 - S_{22}) + S_{12}S_{21}](2S_{21})^{-1}$ and $D(f) = [(1 - S_{11})(1 + S_{22}) + S_{12}S_{21}](2S_{21})^{-1}$.

In accordance to the entire preceded theoretical analysis, the steps of the design are summarized as:

1. It is considered that the lattice is embedded inside a dielectric layer with parameters h_s and ε_{rs} and covered by another dielectric layer of parameters h_c and $\varepsilon_{rc.}$. The values of the parameters are depicted in Table 1 and not changed during the design steps.

2. The side length of the largest among the half dozen patches is calculated in order to resonate around 2 GHz, and initial values for the scale coefficients s and g_s are selected for the evaluation of the size of the rest patches. The calculation is performed using the selected ε_{rs}, ε_{rc} and the theory in [29].

3. A wire dipole with initial length $dip_\ell = \lambda/2$ at 2 GHz (in free space) is positioned in parallel to the lattice, at distance h_d above the middle of focusing cell (Fig. 2(a)).

4. For the selected set of parameter values, two simulations are conducted both with the electromagnetic solver software. One, considering the dipole present but not fed and with two excitation ports, is shown as in Fig. 2(c), and the second one, considering only one feeding port at the input of the dipole. The first simulation gives the values of $S_{ij}(f)$ between the ports, which in turn are used for the calculation of $\beta(f)$, via Eq. (2), and the determination of the frequencies at which it gets zero. The second simulation provides the variation of $S_i(f)$ at the input of the dipole and at the same time the gain of the hybrid antenna.

5. The values of size and inter-distance of the EBG patches governed by s and g_s, the dip_ℓ and h_d are changed through a large number of iterations, and the two simulations are run for every parameter set. The target is to obtain simultaneously a) multiband performance of the EBG, without failing one of them around 2 GHz (UMTS band) and another inside the band of 5–6 GHz (High WiMAX), no matter where the rest of the bands are (if they appear) and b) multiband behavior of the dipole, ascertained by $S_i(f)$, two of them being also at 2 GHz and 5–6 GHz and no matter how many and where other bands of operation will possibly appear.

By the above process it is expected that the best solution found combines multiband operation and focusing which is made sure by high gain values. The most satisfactory solution found is the hybrid antenna with the characteristics presented in Table 1.

The variation of $\beta(f)$ versus frequency of the EBG focusing area-cell (Table 1), as calculated by Eq. (2), is depicted in Fig. 3. It is ascertained that zeroing of $\beta(f)$ occurs at 1.99 GHz, 3 GHz, 3.9 GHz and 5.1 GHz. At these frequencies, resonance performance of the EBG and consequently potential exciting of the dipole are expected. This prediction is verified by simulation of the hybrid radiator via the electromagnetic solver software, and the results are presented in Fig. 4. In Fig. 4(a), the variation of scattering coefficient of the signal at the feeding input of the dipole is depicted for the same structure. For comparison, respective results, received via simulation for half wavelength dipoles in free space and in front of PEC reflector, are also presented. In all three cases, the dipole's length is approximately $\lambda/2$, as proper variations of the typical value are made in order for the dipole to resonate. The results show that the dipole has three clear resonances around the frequencies 2.03 GHz, 3.98 GHz and 5.045 GHz,

which match the results of Fig. 2 very well as these are three out of the four frequencies of $\beta(f)$ zeroing. Regarding 3 GHz, at which $\beta(f)$ also tends to zero, the dipole seems to not respond to the EBG's resonance. Instead, it has a pseudo-resonance at $\sim$ 2.6 GHz. It is also clearly shown that both the dipole in free space and that in front of PEC have just one resonance at 2 GHz coming from the dipole's length.

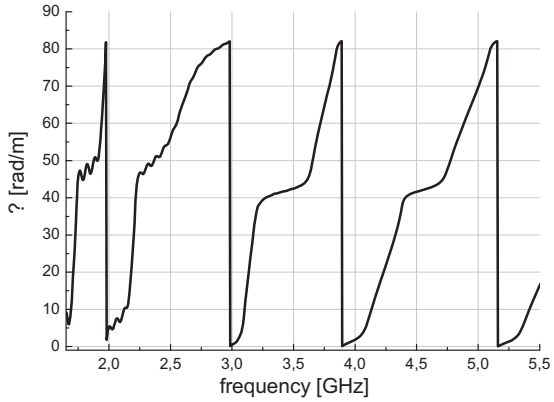

Figure 3. Variation of phase constant versus frequency.

Table 1.

Variables	**Values**
Number of EBG patches/row	6 + their mirror
ε_{rc}	10.2
h_c	1.28 mm
ε_{rs}	2.2
h_s	8 mm
Side length of the largest patch	6.5 mm
s	0.98
g_s	0.98
dip_ℓ	50 mm
h_d	6 mm

The results of Fig. 4(b) illustrate the performance of the dipole in front of the non-uniform EBG (Table 1); however, for three different thickness values of cover dielectric layer, with intention to assess the impact of this parameter on the multi-frequency operation of the entire scheme. It is concluded that this parameter is crucial for both the number and the values of resonance frequencies. At the most thin layer about two resonances between 2 GHz and 2.5 GHz appear, while the scheme with the 1.92 mm cover layer exhibits one resonance around 2 GHz and two additional ones at frequencies different from those of the scheme with the 1.28 mm cover layer. It is also observed that all three hybrid radiators have a resonance around 2 GHz. From all the above results, it is concluded that at this frequency the basic operation mode of the dipole appears. This mode exists with or without the presence of the EBG, due to the dipole's length. The other two resonances (Fig. 4(a)), at the higher frequencies, correspond to new operation modes driven by the EBG. To explain this performance, we have to take into account that when the dipole operates in free space, just fed in the middle of its $\lambda/2$ length, the well-known basic current mode is excited. When it is also fed at the same point, but operates very close to the non-uniform EBG reflector, its current distribution depends not only on its own feeding but also on the power reradiated by the EBG. This interchange of energy constitutes a coupling phenomenon which becomes intense at the EBG's resonances and drives the entire antenna to a performance that will be

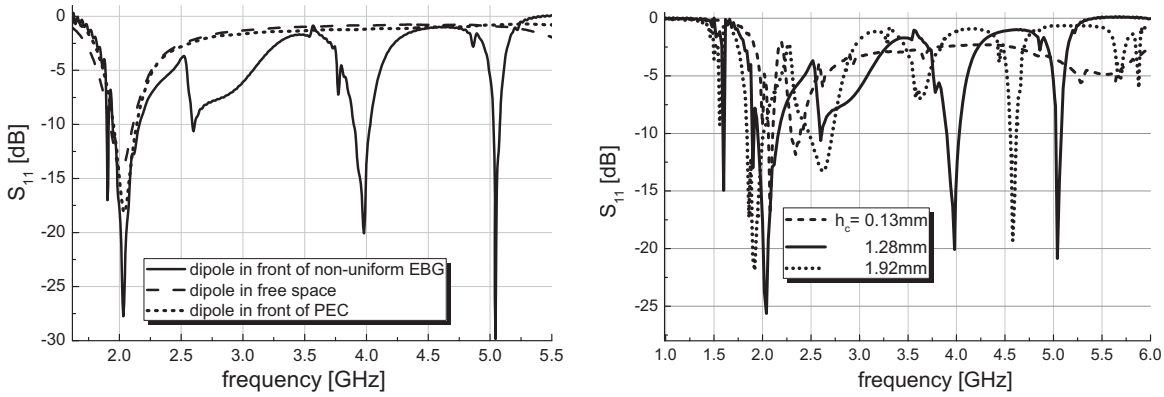

Figure 4. Signal scattering coefficient at the input of the dipole (a) for the scheme of Table 1, in front of PEC and of a single dipole and (b) for the scheme of Table 1 with three different dielectric covers.

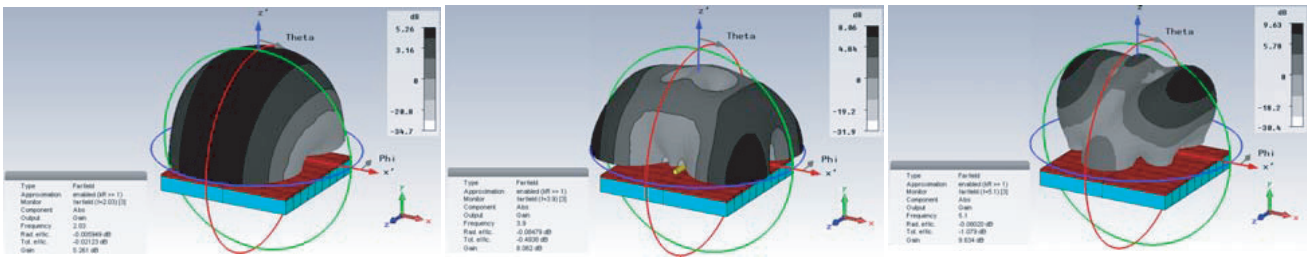

Figure 5. 3D Gain patterns at (a) 2.032 GHz ($G_{\max} = 5.26$ dB), (b) 3.98 GHz ($G_{\max} = 8.06$ dB) and (c) 5.045 GHz ($G_{\max} = 9.6$ dB).

termed as higher order operation mode. The results of Fig. 4(a) validate the response of the dipole to the EBG resonances, for all that it has not the length required for resonance at the respective frequencies in the case of free space. It has also to be pointed out that the sensitivity of the hybrid radiator to the thickness of cover dielectric layer may be considered as an advantage, being an easy way to shift the resonances at bands required from the relative application.

Indicative 3D gain patterns of the scheme at the resonances are depicted in Fig. 5. It is shown that the radiator has gain much greater than that of a single dipole depending on the frequency and reaching 9.6 dB. It is also pointed out that the radiated power does not come only from the dipole. For all that the lattice is a passive scheme, and the dipole is the unique directly fed element. The EBG accepts radiated energy from the dipole, at the frequencies at which the resonated energy is maximized, and the lattice, being substantially a reflector, also radiates. So, what is shown at the 3D patterns is the global radiation of all the hybrid antenna parts. That is why the gain is enhanced

However, this gain index concerns emission or reception of signals of stationary transmitters or receivers. In order for the designed radiator to be useful in contemporary applications as the mobile communication networks, its performance has to be examined in the real environments of this type, at which the characteristics of the propagating signals are of statistical nature. So, instead of the ordinary gain the MEG of the scheme has to be assessed. Another parameter crucial for the effectiveness of the system which the radiator serves, especially in the case of a MIMO one, is the correlation coefficient between the signals at the input of dipoles of the hybrid array. In the work at hand, both these quantities are calculated as function of the parameters of the environment, i.e., the statistical distribution functions and the polarization features of the incoming waves. Analysis and results are presented in the following sections.

3.2. Mean Effective Gain

The Mean Effective Gain G_e of an antenna operating in a multipath environment is an index showing the capability of the antenna to catch the power P_{rec} of a signal following a random route, with respect to the total power $P_V + P_H$, namely of the vertically polarized signals P_V, plus the power of horizontally P_H polarized ones, and is defined as the ratio of these quantities $G_e = P_{rec}/(P_V + P_H)$. The analytical mathematical formula for G_e, which includes both the antenna features of operation and the profile of the incident signals in the real communication environment, is that of Eq. (3) [35].

$$G_e = \int_0^{2\pi}\int_0^{\pi}\left[XPR\,(1+XPR)^{-1}\,G_\theta^{dip-EBG}(\theta,\varphi)P_\theta(\theta,\varphi)+(1+XPR)^{-1}\,G_\varphi^{dip-EBG}P_\varphi\,(\theta,\varphi)\right]\sin\theta d\theta d\varphi \quad (3)$$

where $G_\theta^{dip-EBG}$ and $G_\phi^{dip-EBG}$ are the θ and ϕ components of the gain of the dipole array in front of the EBG; $P_\theta(\theta,\varphi)$ and $P_\phi(\theta,\varphi)$ are respectively the θ and ϕ components of the angular density functions of the incoming plane waves; XPR is the cross-polarization power ratio and equals to P_V/P_H.

The results for MEG of the scheme of Fig. 2 (Table 1) are presented in Fig. 6. They are received via Eq. (3), versus the mean angle of incidence of the incoming waves and for various XPR. For directions of arrival around the mean values, Gaussian distribution is considered, with standard deviation $\sigma = 20$ dB on zy plane and uniform on xy plane. The values of $G_{\theta,\phi}^{dip-EBG}(\theta,\phi)$ are received via simulation of the antenna. For comparison, respective results for dipoles in front of PEC, as reflector, are depicted. It is concluded that the dipole-EBG scheme exhibits levels of MEG higher than that of dipole-PEC, especially at the most usual angles of wave incidence.

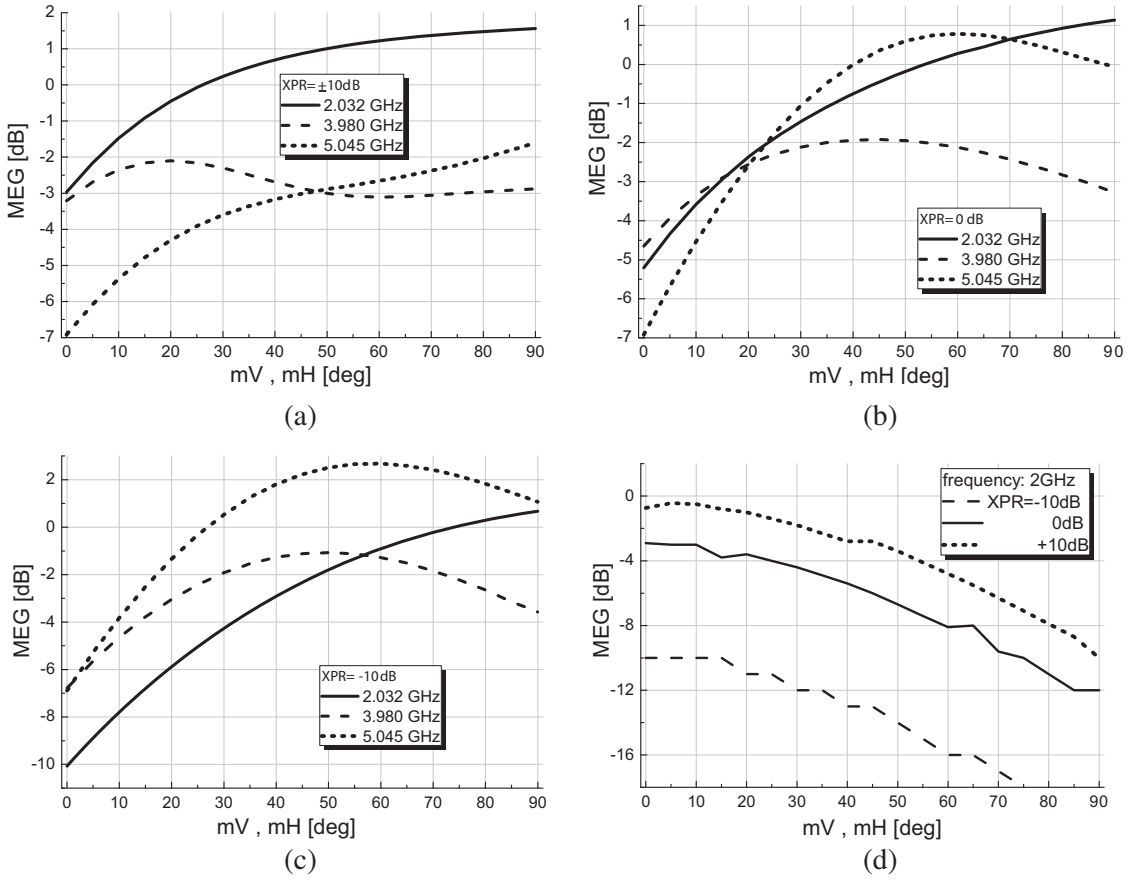

Figure 6. (a), (b), (c) MEG of the scheme of Table 1 for 3 different values of XPR and (d) MEG for the dipole in front of PEC.

3.3. Dual Dipole-EBG Array

The potential to the hybrid radiating unit being used as element in a MIMO array is investigated by estimating the two basic indices MEG and correlation coefficient of a dual-unit hybrid array as shown in Fig. 7(a). One of the units is rotated with respect to the other by 90 deg. So each dipole along with its EBG unit cell is perpendicular to the other, and their electromagnetic coupling is reduced. This reduction is further enhanced by the presence of the non-uniform EBG unit cells.

The results in Fig. 7(b) are about the scattering coefficient of the signal at the input of each dipole and show that both elements hold their multi-frequency operation at the same frequencies. The Mean Effective Gain is calculated as previously, while the correlation coefficient [35] is approximately calculated by the formula ρe; $|Rij|^2(\sigma_i^2\sigma_j^2)^{(-1)}$, and it is the formula of Section 3.3, at the fifth line above Fig. 7, where R_{ij} is the cross-covariance of the voltages induced at the input of the ith and jth elements of the array, calculated by the formula $R_{ij} = 2P_H \int_0^{2\pi}\int_0^{\pi} [XPR \cdot E_{\theta i}(\theta,\varphi)E^*_{\theta j}(\theta,\varphi)P_\theta(\theta,\varphi) + E_{\varphi i}(\theta,\varphi)E^*_{\varphi j}(\theta,\varphi)P_\varphi(\theta,\varphi)]\sin\theta d\theta d\varphi$. σ_i , σ_j are the standard deviations of the complex envelopes of the ith and jth elements of the antenna array, calculated by $\sigma^2_{i,j} = 2P_H \int_0^{2\pi}\int_0^{\pi} [XPR \cdot E_{\theta i,j}(\theta,\varphi)E^*_{\theta i,j}(\theta,\varphi)P_\theta(\theta,\varphi) + E_{\varphi i,j}(\theta,\varphi)E^*_{\varphi i,j}(\theta,\varphi)P_\varphi(\theta,\varphi)]\sin\theta d\theta d\varphi$.

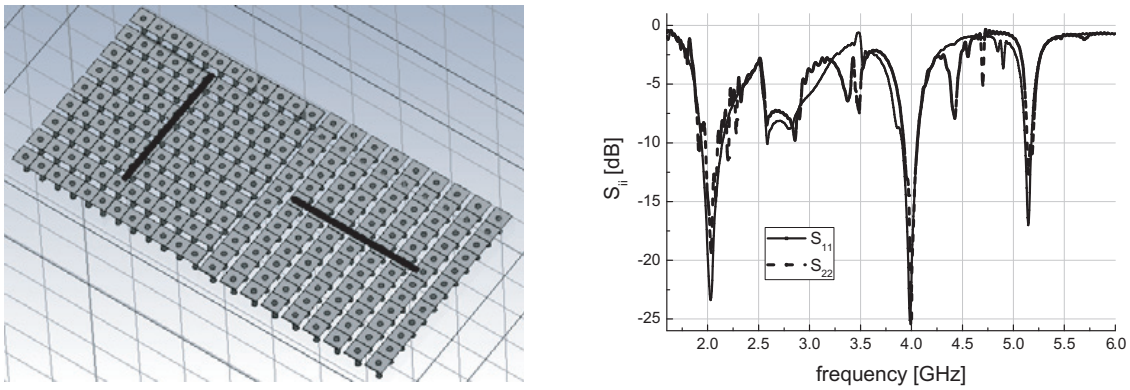

(a) (b)

Figure 7. (a) The dual unit hybrid array, each one along with its dipole, perpendicularly positioned to the other and (b) the signal scattering coefficients at the dipoles' inputs, versus frequency.

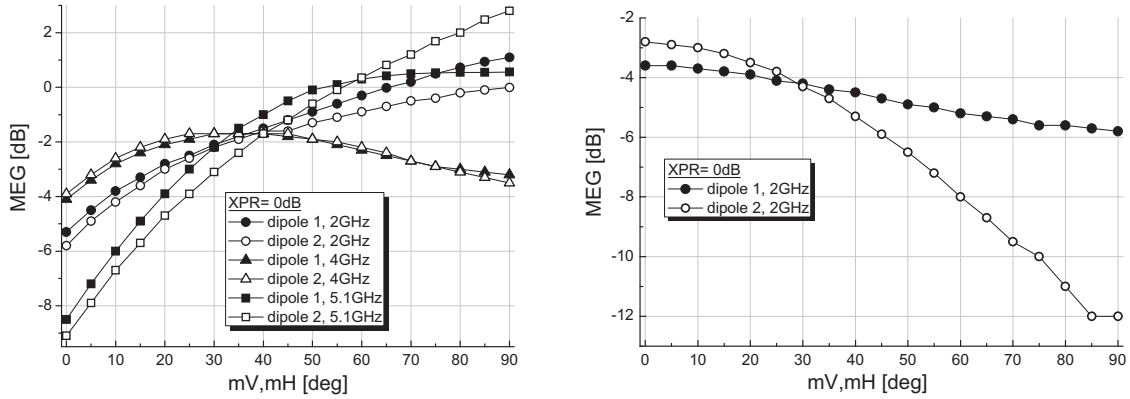

(a) (b)

Figure 8. (a) MEG of both dipoles of the scheme of Fig. 7(a) at the three frequency bands and (b) respective results for the dipoles in front of PEC.

The variation of MEG, of the double-unit structure of Fig. 7(a), versus the angle of incident waves and for various values of XPR is presented in Fig. 8(a). For comparison, respective results for two perpendicular $\lambda/2$ dipoles positioned similarly to those of Fig. 7(a) but at a distance $\lambda/4$ from a PEC surface are depicted in Fig. 8(b). It is shown again that MEG values of the dipole-EBG scheme are satisfactory, larger than those of the dipole-PEC antenna. The correlation coefficient, of the double-unit structure of Fig. 7(a), versus the angle of incident waves and for various values of XPR, is presented in Fig. 9(a), and the respective results of the dipoles in front of PEC are depicted in Fig. 9(b). It is more than obvious that not only the level of correlation of the hybrid array, dipoles-EBG, is much lower than that of the array in front of the PEC, but also these values in all cases are smaller than 0.1.

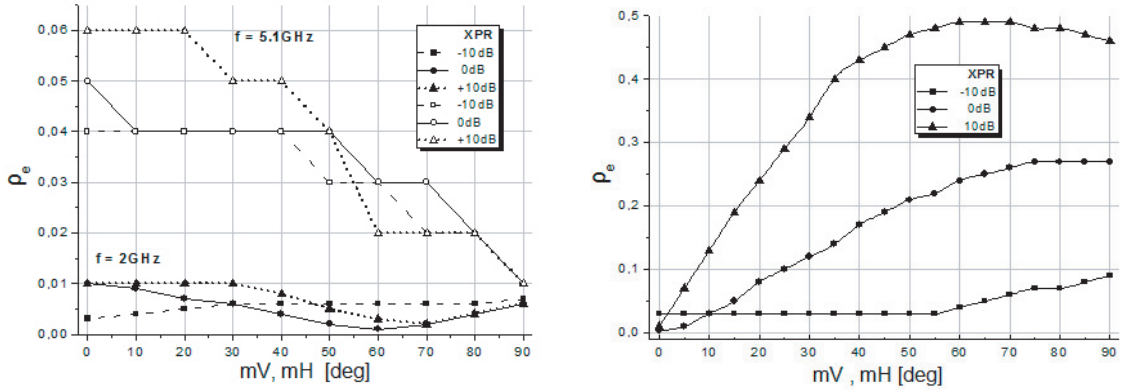

Figure 9. Correlation coefficient versus the mean angle of incidence for various XPR values (a) scheme of Fig. 7(a), (b) the dipoles in front of PEC, at 2 GHz.

4. CONCLUSION

In the present work, a theoretical analysis of the multiband performance of EBG lattices with non-identical cells is carried out, and the possibility of this type of lattices to drive simple antennas, as the wire dipoles, at multiband operation, when positioned in close proximity to them is investigated. It is proved to be feasible and has a new capability of EBGs added to their other, already known, ones. The dipoles have, besides their basic mode of operation coming from their length, higher order resonances which are not excited when they are alone or positioned in front of PEC. This performance is proved via results received for all three types of schemes. The deigned hybrid structure dipole-nonuniform EBG has three bands of operation, with a gain greater than 5 dB and up to 9.6 dB depending on the band. Extensive study is also carried out for indices as MEG and correlation coefficient between the input signals of the dipoles with respect to the mean angle of the impinging waves and their statistical distribution around it, as well as their XPR ratio. The radiator is proved robust giving correlation coefficient values much lower than 0.1 and satisfactory high MEG values, especially when the waves come from the broadside area of the structure. Respective results, received for the classical scheme dipole-PEC, show the definite superiority of the designed hybrid radiator which consequently can be used either as stationary or mobile radiating unit.

REFERENCES

1. Best, S. and D. Hanna, "Design of a broadband dipole in close proximity to an EBG ground plane," *IEEE Antennas and Propagation Magazine*, Vol. 50, 52–64, 2008.
2. Toubet, M. S., M. Hajj, R. Chantalat, E. Arnaud, B. Jecko, T. Monediere, H. Zhang, and J. Diot, "Wide bandwidth, high-gain, and low-profile EBG prototype for high power applications," *IEEE Antennas and Wireless Propagation Letters*, Vol. 10, 1362–1365, 2011.

3. Yuan, T., H. Hafdallah-Ouslimani, A. C. Priou, G. Lacotte, and G. Colligon, "Dual-layer EBG structures for low profile 'bent' monopole antennas," *Progress In Electromagnetics Research B*, Vol. 47, 315–337, 2013.
4. Siakavara, K. and T. Ganatsos, "Modification of the radiation patterns of higher order modes of triangular printed antennas by EBG ground planes," *IEEE Antennas and Wireless Propagation Letters*, Vol. 8, 124–128, 2009.
5. Kim, S.-H., T. T. Nguyen, and J.-H. Jang, "Reflection characteristics of 1-d EBG ground plane and its application to a planar dipole antenna," *Progress In Electromagnetics Research*, Vol. 120, 51–66, 2011.
6. Zhou, L., H. H. Ouslimani, A. Priou, A. Ourir, and O. Maas, "Understanding the behavior of miniaturized metamaterial-based dipole antennas in leky wave regime," *Applied Physics A*, Vol. 106, 145–149, 2012.
7. Hosseini, M., D. M. Klymyshyn, G. Wells, and X. Liu, "Thick metal EBG cells with narrow gaps and application to the design of miniaturized antennas," *Progress In Electromagnetics Research*, Vol. 145, 185–193, 2014.
8. Ganatsos, T., K. Siakavara, and J. N. Sahalos, "Neural network — Based design of EBG surfaces for effective polarization diversity of wireless communications antenna systems," *PIERS Online*, Vol. 3, 1165–1169, 2007.
9. Ganatsos, T., K. Siakavara, and J. N. Sahalos, "Mean effective gain enhancement of antenna systems with EBG ground plane," *Proc. of the 3rd European Conference on Antennas and Propagation*, 3567–3571, Berlin, March 2009.
10. Margaret, D. H., M. R. Subasree, S. Susithra, S. S. Keerthika, and B. Manimegalai, "Mutual coupling reduction in MIMO antenna system using EBG structures," *International Conference on Signal Processing and Communications (SPCOM)*, 2012.
11. Michailidis, E., C. Tsimenidis, and G. Chester, "Mutual coupling reduction in a linear two element patch array and its effect on theoretical MIMO capacity," *Proc. of Louhborough Antennas and Propagation Conference*, 457–460, Louhborough, 2008.
12. Naser-Moghadasi, M., R. Ahmadian, Z. Mansouri, F. B. Zarrab, and M. Rahimi, "Compact EBG structures for reduction of mutual coupling in patch antenna MIMO arrays," *Progress In Electromagnetics Research C*, Vol. 53, 145–154, 2014.
13. Islam, M. T. and Md. Shahidul Alam, "Compact EBG structure for alleviating mutual coupling between patch antenna array elements," *Progress In Electromagnetics Research*, Vol. 137, 425–438, 2013.
14. Yoon, J.-H., J. Ahn, K. Chang, and Y.-J. Yoon, "Beam tilted Base station antenna with electromagnetic gradient surface," *Proc. of International Conference on Electromagnetics in Advanced Applications (ICEAA)*, 481–484, 2010.
15. Chang, K., J. Ahn, and Y.-J. Yoon, "High impedance surface with nonidentical lattices," *Proc. of IWAT2008*, 474–477, Chiba, Japan, 2008.
16. Chang, K. and Y.-J. Yoon, "One-dimensional flat parabola antenna using synthesized EBG textures," *Proc. of IEEE Antennas and Propagation Society International Symposium, APSURSI '09*, 2009.
17. Mourtzios, Ch. and K. Siakavara, "Novel antenna configurations with non-uniform ebg lattices for wireless communication networks," *Proc. of the 7th European Conference on Antennas and Propagation(EuCAP)*, 2673–2677, Gothenburg, April 2013.
18. Mourtzios, Ch. and K. Siakavara, "Hybrid antenna-EBG structures with tunned periodicity for enhancement of operation of wireless networks," *Proc. of International Conference on Electromagnetic Advanced Applications (ICEAA'13)*, 125–128, (file 155.pdf), Turin, September 2013.
19. Mourtzios, Ch. and K. Siakavara, "Hybrid antenna arrays with non-uniform electromagnetic band gap lattices for wireless communication networks," *Indian Journal of Physics*, Vol. 89, 811–823, 2015.

20. Mourtzios, Ch., Th. Ganatsos, and K. Siakavara, "MEG and correlation characteristics of hybrid dipole — Nonuniform EBG antenna systems," *Proc. of the 8th European Conference on Antennas and Propagation (EuCAP2014)*, 3433–3437, Hauge, April 2014.
21. Wu, P., Z. Kuai, and X. Zhu, "Multiband antennas comprising multiple frame-printed dipoles," *IEEE Transactions on Antennas and Propagation*, Vol. 57, 3313–3316, 2009.
22. Peng, L. and Ch. Ruan, "Design and time-domain analysis of compact multi-band-notched UWB antennas with EBG structures," *Progress In Electromagnetics Research B*, Vol. 47, 339–357, 2013.
23. Xu, H.-X., G.-M. Wang, Y.-Y. Lv, M.-Q. Qi, X. Gao, and S. Ge, "Multifrequency monopole antennas by loading metamaterial transmission lines with dual-shunt branch circuit," *Progress In Electromagnetics Research*, Vol. 137, 703–725, 2013.
24. Antoniades, M. A. and G. V. Eleftheriades, "Multiband compact printed dipole antennas using NRI-TL metamaterial loading," *IEEE Transactions on Antennas and Propagation*, Vol. 60, 5613–5626, 2012.
25. Saurav, K., D. Sarkar, and K. V. Srivastava, "CRLH unit-cell loaded multiband printed dipole antenna," *IEEE Antennas and Wireless Propagation Letters*, Vol. 13, 852–855, 2014.
26. Khan, O. M., Z. U. Islam, I. Rashid, F. A. Bhatti, and Q. U. Islam, "Novel miniaturized Koch pentagonal fractal antenna for multiband wireless applications," *Progress In Electromagnetic Research*, Vol. 141, 693–610, 2013.
27. Li, D. and J.-F. Mao, "Circularly arced Koch fractal multiband multimode monopole antenna," *Progress In Electromagnetics Research*, Vol. 140, 653–680, 2013.
28. Siakavara, K. and F. Tsaldaris, "A multi-wideband microstrip antenna designed by the square curve fractal technique," *Microwave and Optical Technology Letters*, Vol. 41, 180–185, 2004.
29. Peristerianos, A., A. Theopoulos, A. G. Koutinos, T. Kaifas, and K. Siakavara, "Dual-band fractal semi-printed element antenna arrays for MIMO applications," *IEEE Antennas and Wireless Propagation Letters*, Vol. 15, 730–733, 2016.
30. Engheta, N. and R. W. Ziolkowski, *Metamaterials_Physics and Engineering Exploriations*, John Wiley & Sons, 2006.
31. Kildal, P.-S., A. A. Kishk, and S. Maci, "Special issue on artificial magnetic conductors, soft/hard surfaces, and other complex surfaces," (Guest Editorial), *IEEE Transactions on Antennas and Propagation*, Vol. 53, No. 1, 2–7, January 2005.
32. Rahmat-Samii, Y. and F. Yang, *Electromagnetic Band Gap Structure in Antenna Engineering*, Cambridge University Press, Cambridge, UK, 2009.
33. Gross, F. B., *Frontiers in Antennas_Next Generation Design & Engineering*, Mc Graw Hill, 2011.
34. Sievenpiper, D., L. Zhang, R. F. J. Broas, N. G. Alexopoulos, and E. Yablonovitch, "High impedance electromagnetic surfaces with a forbidden frequency band," *IEEE Trans. Microwave Theory and Techniques*, Vol. 47, No. 11, 2059–2074, 1999.
35. Pozar, D. M., *Microwave Engneering*, 3rd Edition, John Wiley & Sons, 2005.
36. Fujimoto, K. and J. R. James, *Mobile Antenna Systems Handbook*, Artech House, 2001.